DEVELOPING AN ECO-ROUTING APPLICATION

Final Report

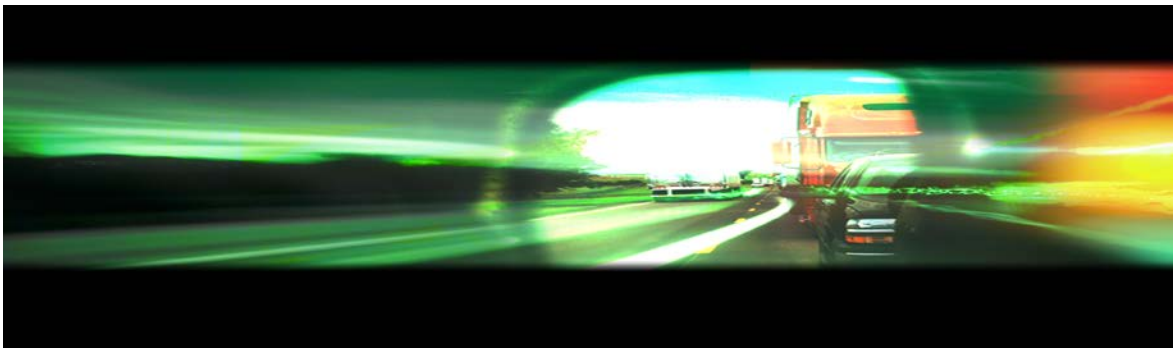

TranLIVE

Hesham Rakha and Kyoungho Ahn

January 2014

DISCLAIMER

The contents of this report reflect the views of the authors, who are responsible for the facts and the accuracy of the information presented herein. This document is disseminated under the sponsorship of the Department of Transportation, University Transportation Centers Program, in the interest of information exchange. The U.S. Government assumes no liability for the contents or use thereof.

1. Report No.	2. Government Accession No.	3. Recipient's Catalog No.
4. Title and Subtitle Developing an Eco-Routing Application		5. Report Date January 2014
		6. Performing Organization Code KLK900-SB-002
7. Author(s) Rakha, Hesham; Ahn, Kyoungho		8. Source Organization Report No. N14-07
9. Performing Organization Name and Address Virginia Polytechnic Institute & State University 1880 Pratt Dr, Suite 2006 Blacksburg, VA 24060		10. Work Unit No. (TRAIS)
Source Organization Name and Address NIATT & TranLIVE University of Idaho 875 Perimeter Dr. MS0901 Moscow, ID 83844-0901		11. Contract or Grant No. DTRT12-G-UTC17
12. Sponsoring Agency Name and Address US Department of Transportation Research and Special Programs Administration 400 7th Street SW Washington, DC 20509-0001		13. Type of Report and Period Covered Final Report: 1/1/2012 – 12/31/2013
		14. Sponsoring Agency Code USDOT/RSPA/DIR-1
15. Supplementary Notes:		

16. Abstract

The study develops eco-routing algorithms and investigates and quantifies the system-wide impacts of implementing an eco-routing system. Two eco-routing algorithms are developed: one based on vehicle sub-populations (ECO-Subpopulation Feedback Assignment or ECO-SFA) and another based on individual drivers (ECO-Individual Feedback Assignment or ECO-IFA). Both approaches initially assign vehicles based on fuel consumption levels for travel at the facility free-flow speed. Subsequently, fuel consumption estimates are refined based on experiences of other vehicles within the same class. This stochastic, multi-class, dynamic traffic assignment framework was demonstrated to work for various scenarios.

This study also quantifies the system-wide impacts of implementing a dynamic eco-routing system, considering various levels of market penetration and levels of congestion in downtown Cleveland and Columbus, Ohio, USA. The study concludes that eco-routing systems can reduce network-wide fuel consumption and emission levels in most cases; the fuel savings over the networks range between 3.3% and 9.3% when compared to typical travel time minimization routing strategies. We demonstrate that the fuel savings achieved through eco-routing systems are sensitive to the network configuration and level of market penetration of the eco-routing system. The results also demonstrate that an eco-routing system typically reduces vehicle travel distance but not necessarily travel time. We also demonstrate that the configuration of the transportation network is a significant factor in defining the benefits of eco-routing systems.

17. Key Words Eco-routing, Eco-driving, fuel consumption estimation, transportation network emission modeling	18. Distribution Statement Unrestricted; Document is available to the public through the National Technical Information Service; Springfield, VT.

19. Security Classif. (of this report) Unclassified	20. Security Classif. (of this page) Unclassified	21. No. of Pages 32	22. Price …

Form DOT F 1700.7 (8-72) Reproduction of completed page authorized

TABLE OF CONTENTS

EXECUTIVE SUMMARY 1
PROBLEM OVERVIEW 2
APPROACH AND METHODOLOGY 4
FINDINGS, CONCLUSIONS AND RECOMMENDATIONS.....10
REFERENCES.....30

EXECUTIVE SUMMARY

The study develops eco-routing algorithms and investigates and quantifies the system-wide impacts of implementing an eco-routing system considering two large metropolitan networks. Recently navigation tools and trip planning services have introduced a vehicle routing option that is designed to minimize vehicle fuel consumption and emission levels, known as eco-routing. The eco-routing option selects the most fuel efficient route, which is not necessarily the shortest distance or the fastest travel time route.

Two eco-routing algorithms are developed: one based on vehicle sub-populations (ECO-Subpopulation Feedback Assignment or ECO-SFA) and another based on individual drivers (ECO-Individual Feedback Assignment or ECO-IFA). Both approaches initially assign vehicles based on fuel consumption levels for travel at the facility free-flow speed. Subsequently, fuel consumption estimates are refined based on experiences of other vehicles within the same class. This stochastic, multi-class, dynamic traffic assignment framework was demonstrated to work for various scenarios.

This study also quantifies the system-wide impacts of implementing a dynamic eco-routing system, considering various levels of market penetration and levels of congestion in downtown Cleveland and Columbus, Ohio, USA. The study concludes that eco-routing systems can reduce network-wide fuel consumption and emission levels in most cases; the fuel savings over the networks range between 3.3% and 9.3% when compared to typical travel time minimization routing strategies. We demonstrate that the fuel savings achieved through eco-routing systems are sensitive to the network configuration and level of market penetration of the eco-routing system. The results also demonstrate that an eco-routing system typically reduces vehicle travel distance but not necessarily travel time. We also demonstrate that the configuration of the transportation network is a significant factor in defining the benefits of eco-routing systems. Specifically, eco-routing systems appear to produce larger fuel savings on grid networks compared to freeway corridor networks. The study also demonstrates that different vehicle types produce similar trends with regard to eco-routing strategies. Finally, the system-wide benefits of eco-routing generally increase with an increase in the level of the market penetration of the system.

This research effort resulted in the following peer-reviewed publications:

1. Rakha H., Ahn K., and Moran K. (2012), INTEGRATION Framework for Modeling Eco-routing Strategies: Logic and Preliminary Results, *International Journal of Transportation Science and Technology*, Vol. 1, No. 3 / September 2012, pp. 259-274, ISSN 2046-0430 (Print), DOI 10.1260/2046-0430.1.3.259
2. Ahn K. and Rakha H. (2013), Network-wide Impacts of Eco-routing Strategies: A Large-scale Case Study, *Transportation Research, Part D: Transport & Environment*, v 25, Dec. 2013, pp. 119–130.

PROBLEM OVERVIEW

Motorists typically choose routes that minimize their travel cost (e.g., travel time). Therefore, drivers typically select longer routes if they produce travel cost savings. The commonly used User Equilibrium (UE) and System Optimum (SO) traffic assignment algorithms utilize minimum travel time or the marginal travel time, respectively as a generalized cost to assign traffic flows over a network. However given that UE and SO assignments are estimated based on travel time, the fuel consumption and emissions of UE and SO conditions may not produce optimum energy and emission levels.

Several researchers have investigated traffic assignment methods using environmental cost functions. Tzeng and Chen (1993) developed the multi-objective traffic assignment method. They formulated multi-objective functions using nonlinear programming techniques and produced various solutions to emit low CO emissions. By utilizing the eigenvector weighting method with pair-wise comparison, the researchers estimated compromised solutions for the flow patterns. They applied the case study of metropolitan Taipei to evaluate the developed traffic assignment model, which utilized a simplified travel time function and CO emission module. The study utilized a fixed amount of CO emissions per link and the total emissions were summed up across all vehicles on a link [1].

Rilett and Benedek (1994) and Benedek and Rilett (1998) investigated an equitable traffic assignment with environmental cost functions. They emphasized the impacts of CO emissions when UE and SO traffic assignments were applied to a sample network, a simple network from Ottawa, Ontario, Canada and a calibrated network from Edmonton, Alberta, Canada. The studies utilized a simple macroscopic CO emission model used in the TRANSYT 7F software. The emission model utilized the average speed and the link length as input variables. The researchers showed that the traffic flows of the SO-CO (the traffic flows that have the minimum total CO emissions) condition were roughly equivalent to the flows of the UE and SO conditions within a small error range [2, 3].

Sugawara and Niemeier (2002) developed an emission-optimized traffic assignment model that used average speed CO emission factors developed by the California Air Resources Board (CARB). The sample network case study concluded that emission-optimized trip assignments can reduce system-level vehicle emissions moderately when compared to the time-dependent UE and SO conditions. The research also found that the emission-optimized assignment is most effective when the network is under low to moderately congested conditions, saving up to 30% of total CO emissions; when the network is highly congested, the emission reduction is diminished to 8%. The authors explain that under emission-optimized conditions, less traffic volume is assigned to the freeway because emission levels are very high at freeway free-flow speeds [4].

Nagurney and her colleagues developed a multi-class and multi-criteria traffic network equilibrium model with an environmental criterion and claimed that a desired environmental quality standard can be achieved by the proposed model through a particular weighting method. In the study, a fixed amount of CO emission rate per traveler per link was utilized to estimate the total CO emissions [5-7].

An earlier study by Ahn and Rakha [8] investigated the impacts of route choice decisions on vehicle energy consumption and emission rates for different vehicle types using microscopic and macroscopic emission estimation tools. The results demonstrated that the faster highway route choice is not always the best route from an environmental and energy

consumption perspective. Specifically, the study found that significant improvements to energy and air quality could be achieved when motorists utilized a slower arterial route although they incurred additional travel time. The study also demonstrated that macroscopic emission estimation tools (e.g. MOBILE6) could produce erroneous conclusions given that they ignore transient vehicle behavior along a route. The findings suggest that an emission- and energy-optimized traffic assignment can significantly improve emissions over the standard User Equilibrium (UE) and System Optimum (SO) assignment formulations. Finally the study demonstrated that a small portion of the entire trip involved high engine-load conditions that produced significant increases in total emissions; demonstrating that by minimizing high-emitting driving behavior, air quality could be improved significantly.

APPROACH AND METHODOLOGY

In order to quantify the system-wide impacts of eco-routing strategies, the study utilizes the INTEGRATION software, which is a microscopic traffic assignment and simulation software [9-12]. A detailed description of the INTEGRATION software logic is beyond the scope of this study but is provided in the literature [13-15]; the simulation framework for modeling eco-routing strategies and test results were described in an earlier publication [16]. The following section describes the fuel consumption and emission models and the eco-routing algorithm implemented in the INTEGRATION software given that they are the two building blocks of the study.

The INTEGRATION software is a microscopic traffic assignment and simulation software [9, 10, 17, 18], conceived as an integrated simulation and traffic assignment model and performs traffic simulations by tracking the movement of individual vehicles every 1/10th of a second. This allows detailed analyses of lane-changing movements and shock wave propagations. It also permits considerable flexibility in representing spatial and temporal variations in traffic conditions. In addition to estimating stops and delays [19-21], the model can also estimate the fuel consumed by individual vehicles, as well as the emissions [22-25]. The model also estimates the expected number of vehicle crashes using a time-based crash prediction model [26]. The INTEGRATION model has not only been validated against standard traffic flow theory [20, 21, 27, 28], but also has been utilized for the evaluation of real-life applications [29-31]. The types of analyses that can be performed with these built-in models extend far beyond the capabilities of EPA's MOBILE6 model [32, 33].

Within the INTEGRATION software, the selection of the next link to be taken by a vehicle is determined by the model's internal routing logic [34-37]. There exist many different variations to the model's basic assignment technique. Some of these techniques are static and deterministic, while others are stochastic and dynamic. However, regardless of the particular technique that is utilized to determine these routings, the selection of the next link that a vehicle should take is done using a vehicle-specific array that lists for the vehicle the entire sequence of links from its origin to its destination. Upon the completion of any link, a vehicle simply queries this array to determine which link it should utilize next to reach its ultimate destination in the most efficient manner. When travel across this next link is in turn completed, the selection process is then repeated until a link whose downstream node is the vehicle's ultimate trip destination is reached. Within the INTEGRATION software five different vehicle classes are specified and each vehicle class can have its unique routing logic. An overview of the various routing logic that is currently provided in the software is described in this section.

Within this traffic assignment process, the key simulation feature to be noted is that turning movements, and therefore all mandatory lane changes, are vehicle-specific and a function of path-based turning movements, rather than based on more arbitrary turning percentages.

The INTEGRATION simulation model currently provides for eight basic traffic assignment/ routing options:

Time-Dependent Method of Successive Averages (MSA)
Time-Dependent Sub-Population Feedback Assignment (SFA)

Time-Dependent Individual Feedback Assignment (IFA)
Time-Dependent Dynamic Traffic Assignment (DTA)
Time-Dependent Frank-Wolf Algorithm (FWA)
Time-Dependent External Routing 1 – File 8 (ER1)
Time-Dependent External Routing 2 – File 9 (ER2)
Distance Based Routing

The first routing mechanism involves the derivation of a time series of MSA traffic assignments. Within this MSA, each time slice is evaluated in isolation of the conditions that prevails either prior or subsequent to the time slice in which the vehicle departs. Furthermore, each vehicle is considered to only affect travel times during the time slice in which the vehicle is scheduled to depart. The link travel times, upon which the route computations are based, are estimated based on the prevailing O-D pattern and an approximate macroscopic travel time relationship for each link. Multiple paths are computed in an iterative fashion where the tree for each subsequent iteration is based on the travel times estimated during the previous iteration. The weight assigned to each new tree is 1/N where N is the iteration number. In other words, the first tree is assigned a weight of 1.0, the second tree a weight of 0.5, and the third tree a weight of 0.333. As weights are added to each new tree, the weight on each previous tree is reduced proportionally.

Routing Mechanism 2 involves the application of a SFA mechanism. Specifically, all drivers within a specific class are divided into five sub populations each consisting of 20% of all drivers within the class. The paths for each of these sub populations are then updated every t seconds during the simulation based on real-time measurements of the link travel times for that specific vehicle class. The value of t is a user-specified value. Furthermore, the minimum path updates of each vehicle sub population are staggered in time, in order to avoid having all vehicle sub populations update their paths at the same time. This results in 20% of the driver paths being updated every $t/5$ s.

Routing Mechanism 3 involves the application of the above feedback mechanism to individual drivers, rather than sub populations. It is referred to as an IFA. The main difference is that, while the paths under Method 2 were always shared by at least 20% of the drivers, within Method 3 all paths are customized to each individual driver and may therefore be unique relative to any other drivers. Given that paths can be computed for individuals, rather than sub populations, the path calculations are triggered based on a vehicle's departure rather than some average time interval as in Method 2 (SFA). In other words, when paths are calculated for sub-populations in Method 2, paths are recomputed for an entire sub-population at specified intervals in anticipation of their subsequent use when vehicles belonging to that sub-population actually depart. This means that paths may often be several seconds, if not minutes old, when a specific vehicle actually departs. In contrast, for Method 3, the path for a specific vehicle is computed at the time of departure of that vehicle. This implies that the paths are computed based on the most recent information that is available at the time of departure.

The default fourth routing mechanism in INTEGRATION involves the use of DTA. This method computes the minimum path for every scheduled vehicle departure, in view of the link travel times anticipated in the network at the time the vehicle will reach these specific links. The anticipated travel time for each link is estimated based on anticipated link

traffic volumes and queue sizes. This routing involves the execution of a complete mesoscopic DTA model prior to the microscopic simulation of the traffic. During this DTA, the routes of all vehicles are computed using the above procedure. Upon completion of this DTA, the actual simulation simply implements the routings computed as per the DTA.

Traffic assignment Method 5 provides for a FWA. It is virtually identical to Method 1 (MSA), except that the weights are optimized rather than set to a default of 1/N. In other words, while the first tree is still assigned a weight of 1.0, the weight on the second tree is optimized rather than set to a default of 0.5. Once the proportion of weights between trees 1 and 2 is set, they are locked in before the weight on the third tree is optimized next. As the weight is added to the third tree, the weights on each of the previous trees are reduced proportionally.

Traffic assignment Methods 6 and 7 provide the user with two opportunities to specify external routings. Specifically, if Routing Method 6 or 7 is specified, vehicles will be routed based on the paths specified in File 8 or 9, respectively, if present. The specified paths in File 8 or 9 can be multi-path and be time-dependent.

Traffic Modeling

Once the routes of travel are selected, the INTEGRATION model updates the vehicle longitudinal and lateral location (lane choice) every deci-second. The longitudinal motion of a vehicle is based on a user-specified steady-state speed-spacing relationship and the speed differential between the subject vehicle and the vehicle immediately ahead of it. In order to ensure realistic vehicle accelerations, the model uses a vehicle dynamics model that estimates the maximum vehicle acceleration level. Specifically, the model utilizes a variable power vehicle dynamics model to estimate the vehicle's tractive force that implicitly accounts for gear-shifting on vehicle acceleration. The model computes the vehicle's tractive effort, aerodynamic, rolling, and grade-resistance forces, as described in detail in the literature [13, 14].

The car-following model is formulated as:

$$u_n(t+\Delta t) = \min\left\{\begin{array}{l} u_n(t) + a_n\left(t\right)\Delta t, \\ \dfrac{-c_1' + c_3 u_f + \tilde{s}_n(t) - \sqrt{\left[c_1' - c_3 u_f - \tilde{s}_n(t)\right]^2 - 4c_3\left[\tilde{s}_n(t)u_f - c_1' u_f - c_2\right]}}{2c_3} \end{array}\right\} \qquad (1)$$

The model constants are computed as

$$c_1' = \frac{u_f}{k_j u_c^2}\left(2u_c - u_f\right) + \max\left(\frac{u_n^2\left(t\right) - u_{n-1}^2\left(t\right)}{2d}, 0\right); \quad c_2 = \frac{u_f}{k_j u_c^2}\left(u_f - u_c\right)^2; \quad c_3 = \frac{1}{q_c} - \frac{u_f}{k_j u_c^2};$$

and the vehicle spacing is computed as:

$$\tilde{s}_n(t) = x_{n-1}(t) - x_n(t) + \left[u_{n-1}(t+\Delta t) - u_n(t)\right]\Delta t + 0.5a_{n-1}(t+\Delta t)\Delta t^2 .$$

Here $u_n(t+\Delta t)$ is the speed of the following vehicle (vehicle n) at time $t+\Delta t$; $a_n(t)$ is the acceleration of the subject vehicle (vehicle n); u_f is the roadway mean free-flow speed; u_c is the roadway mean speed-at-capacity; q_c is the roadway mean capacity; k_j is the roadway

mean jam density; $x_n(t)$ is the position of the subject vehicle at time t; and $x_{n-1}(t)$ is the position of the lead vehicle at time t. This model ensures that the vehicle acceleration does not exceed the vehicle dynamics maximum acceleration level.

The lane selection and lane-changing logic was described and validated against field data in an earlier publication [15]. A later study [38] demonstrated the validity of the INTEGRATION software for estimating the capacity of weaving sections by comparing the software to field-observed weaving section capacities.

Estimation of Vehicle Fuel Consumption and Emission Levels

The INTEGRATION model computes a number of measures of effectiveness (MOEs), including the average speed; vehicle delay; person delay; fuel consumed; vehicle emissions of carbon dioxide (CO_2), carbon monoxide (CO), hydrocarbons (HC), oxides of nitrogen (NO_x), and particulate matter (PM) in the case of diesel engines; and the vehicle crash risk and severity.

The computation of deci-second speeds permits the steady-state fuel consumption rate for each vehicle to be computed each second on the basis of its current instantaneous speed and acceleration level [22-25, 33, 39]. The VT-Micro model was developed as a statistical model from experimentation with numerous polynomial combinations of speed and acceleration levels to construct a dual-regime model as described in Equation (2), where $L_{i,j}$ are model regression coefficients at speed exponent i and acceleration exponent j, $M_{i,j}$ are model regression coefficients at speed exponent i and acceleration exponent j, v is the instantaneous vehicle speed in kilometers per hour (km/h), and a is the instantaneous vehicle acceleration (km/h/s). These fuel consumption and emission models were developed using data that were collected on a chassis dynamometer at the Oak Ridge National Labs (ORNL), data gathered by the Environmental Protection Agency (EPA), and data gathered using an on-board emission measurement device (OBD). These data included fuel consumption and emission rate measurements (CO, HC, and NO_x) as a function of the vehicle's instantaneous speed and acceleration levels. The VT-Micro fuel consumption and emission rates were found to be highly accurate compared to the ORNL data, with coefficients of determination ranging from 0.92 to 0.99. A more detailed description of the model derivation is provided in the literature [40].

$$F(t) = \begin{cases} \exp\left(\sum_{i=1}^{3}\sum_{j=1}^{3} L_{i,j} v^i a^j\right) & \text{for } a \geq 0 \\ \exp\left(\sum_{i=1}^{3}\sum_{j=1}^{3} M_{i,j} v^i a^j\right) & \text{for } a < 0 \end{cases} . \qquad (2)$$

From a general point of view, the use of instantaneous speed and acceleration data for the estimation of energy and emission impacts of traffic improvement projects provide a major advantage over state-of-practice methods that estimate vehicle fuel consumption and emissions based exclusively on the average speed and number of vehicle-miles traveled by vehicles on a given transportation link.

Proposed Eco-routing Logic

Two eco-routing algorithms were added to the INTEGRATION routing logic. These algorithms correspond to routing methods 9 and 10. Routing method 9 is very similar to routing method 2 while routing method 10 is similar to 3 except that the objective function is to minimize a vehicle's fuel consumption level as opposed to its travel time. The two new routings are described in detail in this section.
Initially, when the network is empty routes are selected by computing the vehicle fuel consumption level for each link based on travel at the facility's free-flow speed considering the grade on the link. The fuel consumption rate for a cruising speed equal to the free-flow speed and a grade of G can be computed as

$$F(t) = \exp\left(\sum_{i=1}^{3}\sum_{j=1}^{3} L_{i,j} v_f^i \left(gG\right)^j\right). \quad (3)$$

Here $F(t)$ is the fuel consumption rate (l/s); g is the gravitational acceleration (9.8067 m/s^2) and G is the roadway grade (dimensionless).

The total fuel consumed on the link can then be estimated as

$$F_l = 3600 \times F(t) \times \frac{d_l}{\left(v_f\right)_l} \quad \forall\, l. \quad (4)$$

Here F_l is the total fuel consumed on link l (liters); d_l is the length of link l (km); and $(v_f)_l$ is the free-flow speed on link l (km/h).

Following the initial vehicle routing, vehicles record their fuel consumption experiences prior to exiting a link. A moving fuel consumption estimate for each link in the network is created as

$$F'^{t}_{l,c} = \alpha F^{t}_{l,c} + \left(1-\alpha\right) F'^{t-\Delta t}_{l,c}. \quad (5)$$

Here $F'_{l,c}$ is the smoothed fuel consumption estimate for vehicle class c on link l at instant t; α is a user specified smoothing constant in the interval [0,1]; $F^{t}_{l,c}$ is the observed fuel consumption estimate for vehicle class c on link l at instant t; and $F'^{t-\Delta t}_{l,c}$ is the smoothed fuel consumption estimate for vehicle class c on link l at instant t-Δt.

Errors in the fuel consumption estimates can also be introduced using a white noise error function as

$$F''^{t}_{l,c} = F'^{t}_{l,c} + w_c. \quad (6)$$

Where $F''_{l,c}$ is the final fuel consumption level of vehicle class c on link l at instant t and w_c is a user-specified white noise error in the fuel consumption estimates. This error term is either normally or log-normally distributed with a mean of zero and a user specified coefficient of variation (ratio of standard deviation to mean fuel consumption measurement). The introduction of random errors allows for the modeling of stochastic user equilibrium where different sub-populations or drivers have different minimum paths.

ECO-Sub-population Feedback Assignment

Routing Mechanism 9 involves the application of an ECO-SFA mechanism, however in this case the minimum path is based on the fuel consumption experiences of other drivers within the same class. Specifically, all drivers within a specific class are divided into five sub populations each consisting of 20% of all drivers within the class. The paths for each of these sub populations are then updated every *t* seconds during the simulation based on real-time measurements of the link fuel consumption levels for that specific vehicle class. As was the case with routing mechanism 2, the value of *t* is a user-specified value. Furthermore, the minimum path updates of each vehicle sub population are staggered in time, in order to avoid having all vehicle sub populations update their paths at the same time. This results in 20% of the driver paths being updated every *t*/5 s.

ECO-Individual Feedback Assignment

Routing mechanism 10 involves the application of the above feedback mechanism to individual drivers, rather than sub populations. It is referred to as an ECO-IFA. The main difference is that, while the paths under method 9 were always shared by at least 20% of the drivers, within method 10 all paths are customized to each individual driver and may therefore be unique relative to any other drivers. Given that paths can be computed for individuals, rather than sub populations, the path calculations are triggered based on a vehicle's departure rather than some average time interval as in method 9 (ECO-SFA). In other words, when paths are calculated for sub-populations in method 9, paths are recomputed for an entire sub-population at specified intervals in anticipation of their subsequent use when vehicles belonging to that sub-population actually depart. This means that paths may often be several seconds, if not minutes old, when a specific vehicle actually departs. In contrast, for method 10, the path for a specific vehicle is computed at the time of departure of that vehicle from its origin and from each link. This implies that the paths are computed based on the most recent information that is available at that time. It should also be noted that the selection of the next link that a vehicle should take is done using a vehicle-specific array that lists for that vehicle the entire sequence of links from its origin to its destination. Upon the completion of any link, a vehicle simply submits its experiences fuel consumption on the link and then queries this array to determine which link it should utilize next to reach its ultimate destination in the most efficient manner. When travel across this next link is in turn completed, the updating and selection process is then repeated until a link whose downstream node is the vehicle's ultimate trip destination is reached. Again as was mentioned earlier, the vehicle only uses the experiences of other vehicles in the same class to update the fuel consumption estimates on a link. This allows for a multi-class, stochastic , dynamic, ECO-routing user equilibrium. The routing is multi-class because vehicles are only affected by experiences of other vehicles in the same class. The routing is dynamic because the vehicle can change its route while en-route as traffic conditions change.

FINDINGS, CONCLUSIONS AND RECOMMENDATIONS

The eco-routing algorithm was tested on a sample network composed of two alternative routes for travel from zone 1 to zone 2 (squared nodes), as illustrated in Figure 1. The first route involved travel along an arterial route (path 1→3→5→2), while the second path involved travel along a combination of arterial and freeway travel (path 1→3→4→5→2). Links 1, 2, and 5 were arterials with a free-flow speed of 77 km/h while links 3 and 4 were freeway links with a free-flow speed of 100 km/h. The speed-at-capacity on the arterial and freeway facilities were set approximately equal to the free-flow speed (76 and 99 km/h, respectively) in order to ensure that the average speed did not vary as a function of the level of congestion on the roadway. All links were 0.5 km long except for link 2, which was 1.0 km long, in order to ensure that both paths were of equal length (2 km). All vehicles would travel on the arterial route to node 3 and then would have two equal distance choices: a slower arterial route (link 2) or a faster freeway route (links 3 and 4). The two routes then meet at node 5 and vehicles travel the remainder of the trip along the arterial facility (link 5).

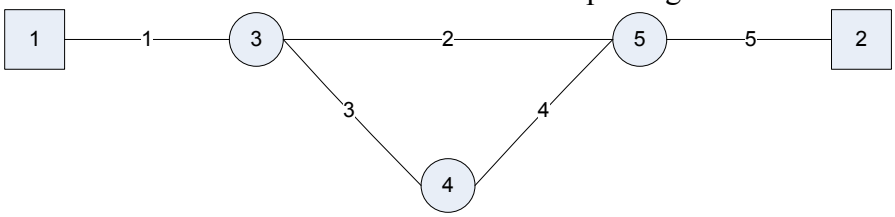

Figure 1: Sample Network Configuration

The optimum fuel consumption rate can be derived by taking the derivative of Equation (2) with respect to speed and setting it equal to zero as demonstrated in Equation (7). If the grades on the roadways are zero Equation (7) is simplified as demonstrated in Equation (8). The speed that produces the minimum vehicle fuel consumption (optimum speed) for the average ORNL vehicle is 76.6 km/h.

$$\begin{aligned}&\left(L_{1,\,0}+L_{1,\,1}a\ +\ L_{1,\,2}a^2+\ L_{1,\,3}a^3\right)v_{opt}+2\left(L_{2,\,0}+L_{2,\,1}a\ +L_{2,\,2}a^2+L_{2,\,3}a^3\right)v_{opt}^2\\&+3\left(L_{3,\,0}+L_{3,\,1}a+L_{3,\,2}a^2+L_{3,\,3}a^3\right)v_{opt}^3=1\end{aligned} \tag{7}$$

$$L_{1,\,0}v_{opt}+2L_{2,\,0}v_{opt}^2+3L_{3,\,0}v_{opt}^3-1=0 \tag{8}$$

The variation in vehicle fuel consumption levels for the ORNL composite vehicle to travel along a 1-km section of roadway as a function of the vehicle cruise speed is illustrated in Figure 2. The figure demonstrates that the shape of the function is a bowl shape with the minimum fuel consumption rate of 0.0777 L/km occurring at a cruise speed of 76.65 km/h. The fuel consumption rate relative to the minimum rate is 1.07 for a cruise speed of 100 km/h (i.e. travel at 100 km/h results in a 7 percent increase in the fuel consumption rate), as demonstrated in Figure 2(b) and Table 1.

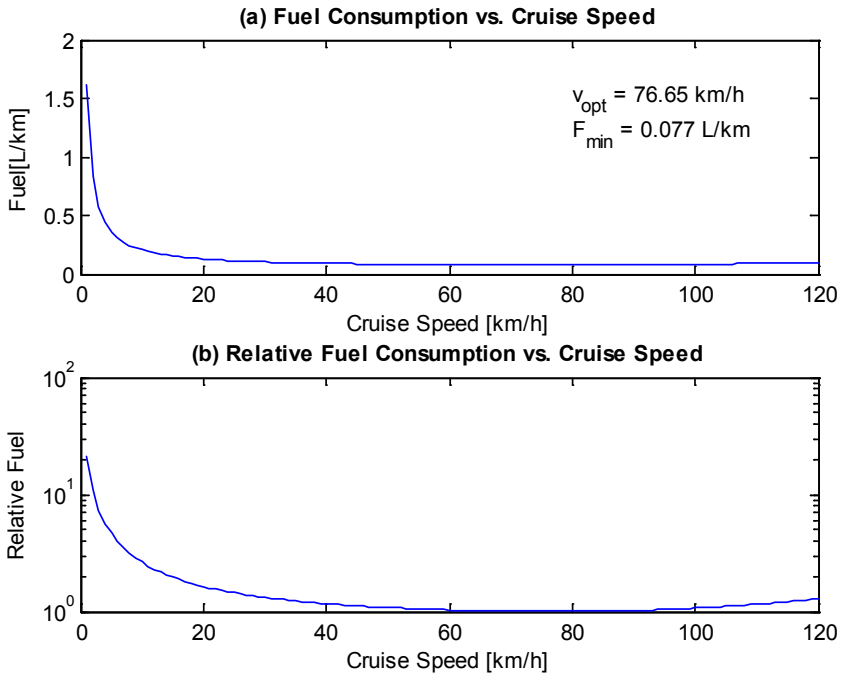

Figure 2: Variation in Fuel Consumption as a Function of Cruise Speed (a) Fuel Consumption; (b) Fuel Consumption Relative to Optimum Fuel Consumption

Table 1: Variation in Relative Fuel Consumption as a Function of Cruise Speed

v (km/h)	F/F_{min}	v (km/h)	F/F_{min}	v (km/h)	F/F_{min}	v (km/h)	F/F_{min}
70	1.005	80	1.001	90	1.021	100	1.070
71	1.004	81	1.002	91	1.025	101	1.077
72	1.002	82	1.003	92	1.029	102	1.084
73	1.001	83	1.005	93	1.033	103	1.092
74	1.001	84	1.006	94	1.037	104	1.099
75	1.000	85	1.008	95	1.042	105	1.108
76	1.000	86	1.010	96	1.047	106	1.117
77	1.000	87	1.013	97	1.052	107	1.126
78	1.000	88	1.015	98	1.058	108	1.136
79	1.001	89	1.018	99	1.064	109	1.146

Consequently, from a travel time perspective it would be more efficient to travel along the freeway roadway while from a fuel economy perspective it would be more efficient to travel along the arterial.

A total demand of 1200 veh/h traveling from zone 1 to 2 was loaded onto the network for the first 1200 seconds. The simulation was continued until all vehicles cleared the network. This resulted in a total of 400 vehicles being simulated, as summarized in Table 2.

Each of the scenarios constitutes four runs: Scenario 1 includes runs 3 through 6 while Scenario 2 includes runs 7 through 10. The runs reflect four routing strategies, as follows:

a. Runs 3 and 7 model the proposed time-dependent sub-population feedback eco-routing logic (ECO-SFA or routing method 9);
b. Runs 4 and 8 model the time-dependent sub-population feedback user equilibrium logic (SFA or routing method 2);
c. Runs 5 and 9 model the proposed time-dependent individual feedback eco-routing logic (ECO-IFA or routing method 10); and
d. Runs 6 and 10 model the time-dependent individual feedback assignment (IFA or routing method 3).

Table 2: Summary Results for Scenarios 1 and 2

Measure	Run 3	Run 4	Run 5	Run 6	Run 7	Run 8	Run 9	Run 10
Total Demand	400	400	400	400	400	400	400	400
Total Travel Distance (veh-km)	799	798	799	798	798	798	799	798
Total Vehicle Stops	30	97	0	97	93	0	95	0
Total Travel Time (veh-s)	36862	33401	37321	33401	32832	28680	33440	28680
Total Stopped Delay (veh-s)	0	0	0	0	0	0	0	0
Total Decel/Accel Delay (veh-s)	166	435	1	435	442	0	432	0
Total Fuel Consumption (veh-L)	65	76	62	76	76	66	77	66
Total HC Emissions (veh-g)	101	312	47	312	295	58	312	58
Total CO Emissions (veh-g)	2267	8414	729	8414	7769	1037	8422	1037
Total NOx Emissions (veh-g)	147	219	129	219	226	227	221	227
Total CO2 Emissions (veh-g)	148412	165014	143207	165014	166546	153194	166854	153194
Avg. Distance (km)	2.00	2.00	2.00	2.00	2.00	2.00	2.00	2.00
Avg. Stops	0.07	0.24	0.00	0.24	0.23	0.00	0.24	0.00
Avg. Travel Time (s)	92.16	83.50	93.30	83.50	82.08	71.70	83.60	71.70
Avg. Stopped Delay (veh-s)	0.00	0.00	0.00	0.00	0.00	0.00	0.00	0.00
Avg. Decel/Accel Delay (veh-s)	0.42	1.09	0.00	1.09	1.11	0.00	1.08	0.00
Avg. Fuel Consumption (L)	0.16	0.19	0.15	0.19	0.19	0.17	0.19	0.17
Avg. HC Emissions (g)	0.25	0.78	0.12	0.78	0.74	0.14	0.78	0.14
Avg. CO Emissions (g)	5.67	21.03	1.82	21.03	19.42	2.59	21.05	2.59
Avg. NOx Emissions (g)	0.37	0.55	0.32	0.55	0.57	0.57	0.55	0.57
Avg. CO2 Emissions (g)	371.03	412.53	358.02	412.53	416.37	382.98	417.14	382.98

Scenario 1: Arterial with Freeway Diversion

In scenario 1 links 1 and 5 were arterial links and would be typical of driver's commute where one typically starts on lower facility roadways and then has the option to travel on a freeway or continue travel on the lower facility roadway. Both options then entail traveling on the lower facility roadway to reach their destination.

As demonstrated in the results of Table 2 that routing methods 2 and 3 (runs 4 and 6) result in all vehicles taking the freeway route in order to minimize the driver travel times. This route, however results in an average fuel consumption of 0.19 L/veh.

Alternatively, when vehicles are routed using the routing mechanism 9 (run 3) one of the sub-populations uses route 2 (freeway route) for the initial update horizon (first 300 s), as illustrated in Figure 3. The majority of vehicles use route 1 (arterial route) and all vehicles

use route 1 after vehicle feedback is received. Figure 3(a) shows the initial oscillations in experienced travel times depending on the route of choice. In the case travel along links 1 and 5 is 48 s while travel along the parallel freeway section is 36 s (travel along links 3 and 4) and travel along the parallel arterial is 46.8 s (link 2). The total travel time along the arterial/freeway route (route 2: links 1, 3, 4, and 5) is 82.8 s while travel along the arterial route is 93.5 s (route 1: links 1, 2, and 5), as illustrated in Figure 3(b). As demonstrated in Figure 3(c) travel along route 2 results in a higher fuel consumption level compared to route 1. It should be noted that some vehicles that travel along route 1 experience higher fuel consumption levels because of the congestion that forms upstream of the diverge point at node 3. This routing mechanism reduces the vehicle fuel consumption level from 0.19 to 0.16 L for the entire trip (see Table 2), which corresponds to a 15 percent reduction in the average fuel consumption level. This saving in fuel consumption comes at an increase of 10 percent in travel time (92.6 versus 83.5 s).

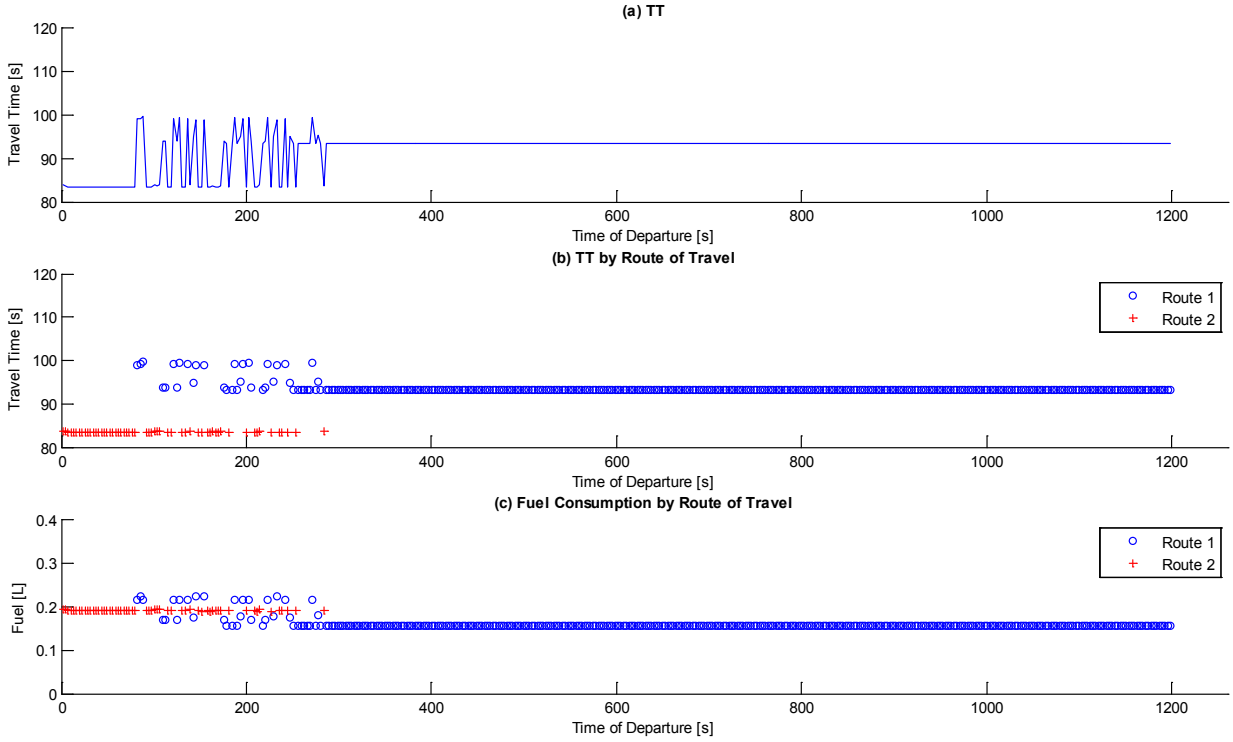

Figure 3: Run 3 Temporal Variation in Individual Vehicle Travel Time and Fuel Consumption Levels

When vehicles are routed using the ECO-IFA mechanism all vehicles travel along route 1, as illustrated in Figure 4. This results in a further reduction in the vehicle fuel consumption level from 0.16 L for the ECO-SFA mechanism to 0.15 L for the ECO-IFA mechanism, as summarized in Table 2.

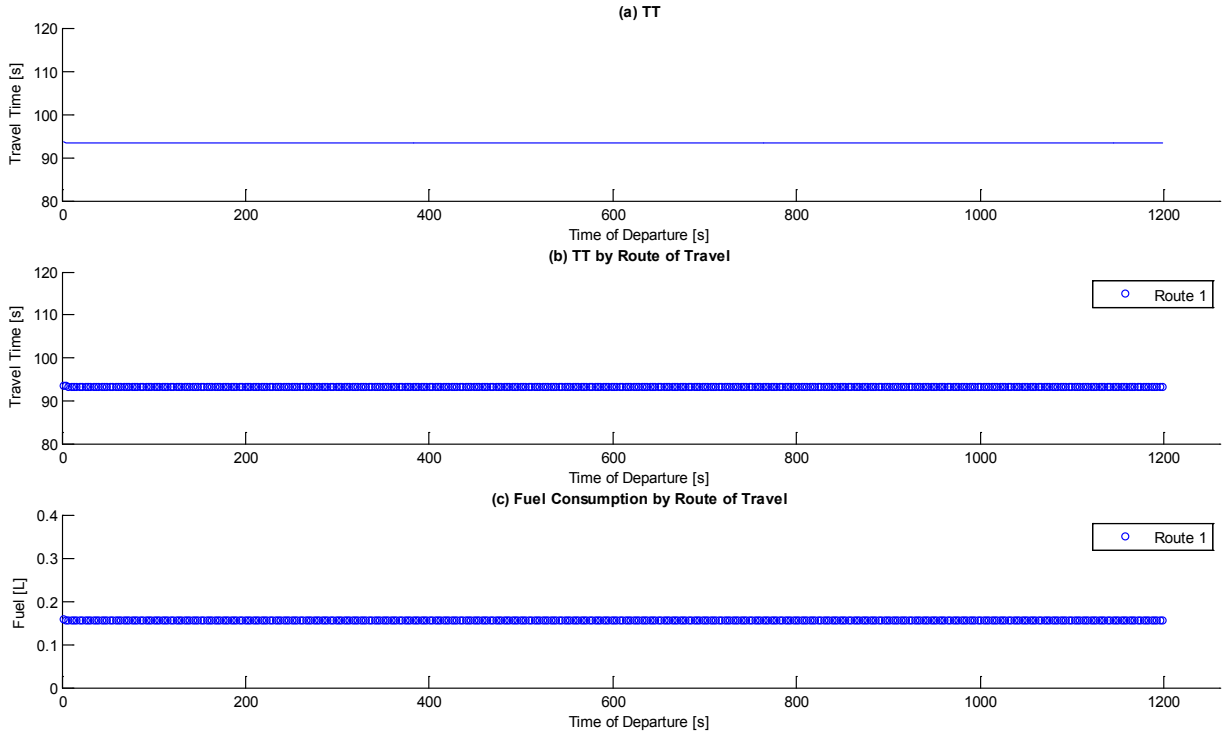

Figure 4: Run 5 Temporal Variation in Individual Vehicle Travel Time and Fuel Consumption Levels

Scenario 2: Freeway with Arterial Diversion

In scenario 2 links 1 and 5 are made freeway links instead of arterial links and thus the free-flow speed on links 1 and 5 are 100 km/h instead of 77 km/h as was the case in Scenario 1. This example, entails traveling on a freeway and having the option to continue on the freeway or exit the freeway to travel on a slower but more fuel efficient arterial roadway.

As was the case in Scenario 1, the SFA and IFA routing strategies would entail continuing to travel on the freeway roadway (traveling on links 3 and 4). This produces an average travel time of 71.7 s. In the case of ECO-IFA (run 9) all 400 drivers select the more efficient arterial route (route 1). The vehicles increase their average travel time from 71.7 s to 83.6 s, as would be expected. However, what is not expected is that the average fuel consumption actually increases from 0.17 to 0.19 L by selecting the more fuel efficient arterial route. This increase in fuel consumption, while might appear counter intuitive as first glance, results from the fact that vehicles the vehicles that enter the freeway from the more efficient arterial route have will accelerate from a speed of 77 km/h to 100 km/h on link 5. Consequently, although the drivers select the more fuel efficient route they incur and acceleration penalty on the freeway and thus increase their overall fuel consumption level. Had the length of the arterial and freeway routes been slightly longer the savings in fuel consumption would have outweighed the penalty associated with the vehicle accelerations on the freeway on link 5.

Simulation Study

This section investigates the impact of eco-routing using two sample networks (downtown Cleveland and Columbus), as illustrated in Figure 5. Both networks were initially constructed to evaluate transportation operational strategies of the downtowns of Cleveland, OH, and Columbus, OH.

There are several advantages to using the selected networks. Firstly, both networks reflect real-world traffic conditions in large metropolitan areas under typical peak demand levels. Secondly, each network contains a range of road types, including multiple interstate highways, highway ramps, major arterials, and local connectors. Thirdly, the network includes traffic control infrastructure such as stop signs and traffic signals using optimized signal timing plans. It should be noted that actual traffic signal timing data were coded in the simulation model.

The Cleveland network includes four interstate highways (I-90, I-71, I-77, and I-490) that serve the downtown area of Cleveland, OH. The network is composed of more than 2,900 links with a traffic demand of 65,000 vehicles in one hour during the morning peak hour. The diagonally shaped I-90 connects the east and west sides of Cleveland and connects to other interstate highways (I-71, I-77, and I-490). The Cleveland network was constructed using 1,397 nodes, 2,985 links, 209 traffic signals, and 8,269 origin-destination (O-D) demand pairs using the 2010 traffic demand data.

The Columbus network comprises three interstate highways (I-70, I-71, and I-670) and is bisected by two interstate highways (I-70 running east to west and I-71 running north to south). The downtown area, which comprises the three interstates, is a major traffic congestion point during rush hours. The shape of the Columbus network is a grid configuration. This network provides more opportunities for re-routing compared to the Cleveland network. The Columbus network was constructed using 2,056 nodes, 4,202 links, 254 traffic signals, and 21,435 O-D demand pairs based on 2010 demand data.

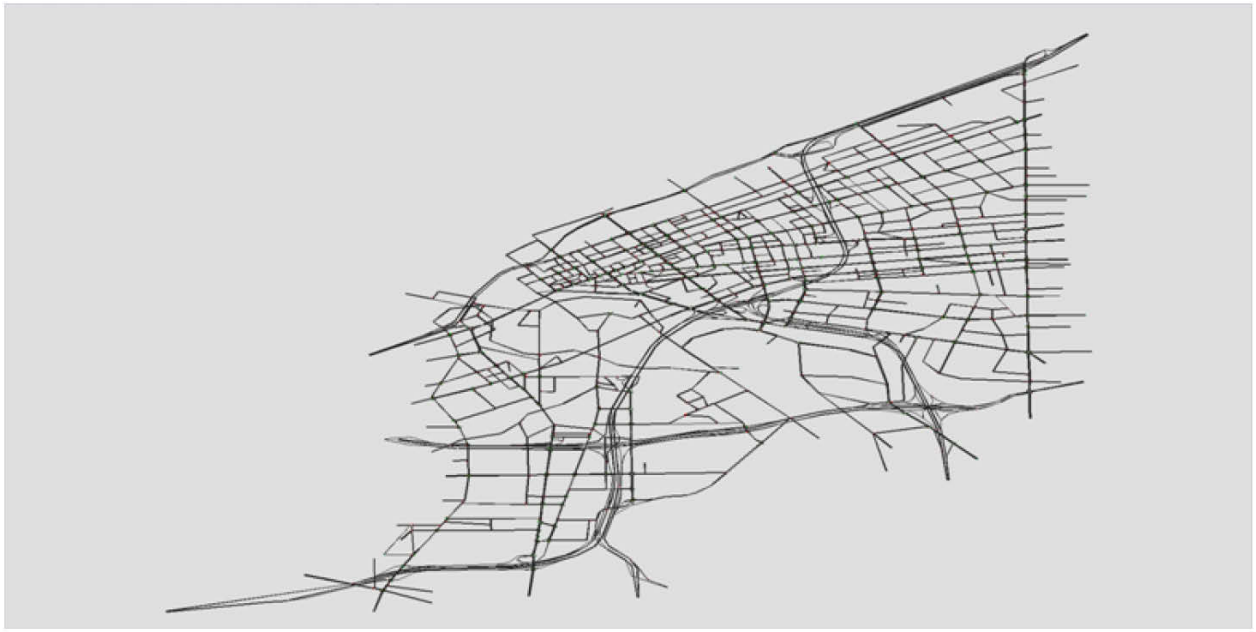

(a) Cleveland Network

(b) Columbus Network

Figure 5: Sample network configuration.

Eco-Routing of Specific Origin and Destination (O-D) Pairs

The first step in the analysis entailed evaluating the performance of eco-routing strategies relative to state-of-the-practice minimum travel time routing algorithms (or TT-routing). The TT-routing uses a dynamic UE algorithm to provide a minimum travel time for each vehicle on the network. A single vehicle type (the ORNL composite vehicle type), which is a composite vehicle including gasoline-powered light-duty vehicles and light-duty trucks, was employed in the analysis. A detailed description of the vehicle is provided elsewhere [41]. The TT-routing involves the use of a dynamic traffic assignment method. Every vehicle estimates the minimum travel time path using the link travel times anticipated in the network at the time the vehicle will reach these specific links. This method generates a routing that is typical of navigation tools.

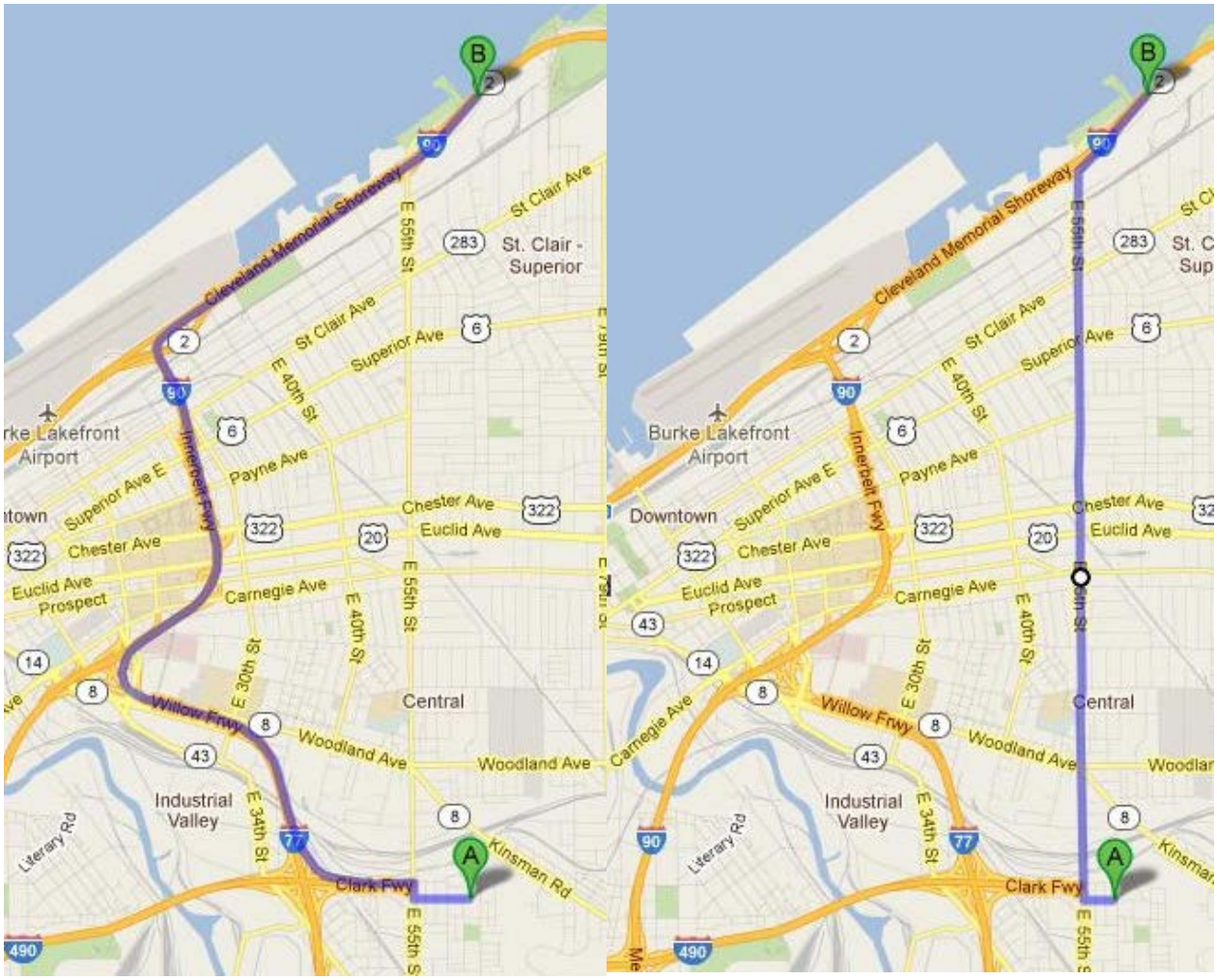

(a) Shortest Travel Time Route (b) Eco-Route

Figure 6: Vehicle Routing Test on Cleveland Network (Source – 2012 Google Map)

Figure 6 illustrates the two routing options on the Cleveland network when vehicles depart from the intersection of Francis Avenue and East 61st Street and arrive to Exit 175 on Interstate 90. The origin and the destination are represented by the letters A and B in the figure, respectively. In case of the eco-routing option, vehicles mainly use E 55th Street as shown in the figure, while vehicles use a highway route (I-77 north and I-90 East) when the TT-routing is used. It should be noted that all the vehicles on the network depart from the origin and arrive at the destination in order to ensure that the results are reported for the same total demand.

Table 3 demonstrates the summary of one-hour simulation results with a demand of 800 veh/h. The result shows that TT-routed vehicles find a shorter travel time route while eco-routed vehicles reduce their fuel consumption by 18 percent compared to the TT-routing option. In particular, TT-routed vehicles use a longer but shorter travel time route. Specifically, they travel 9.83 km and take 409 seconds while the trip distance of eco-routed

vehicles is 7.22 km and spend 591 seconds traveling. TT-routed vehicles travel a distance approximately 27 percent longer with a 44 percent reduction in total travel time. Alternatively, while the eco-routed vehicles increase their travel time by approximately 3 minutes, they reduce their fuel consumption by 18 percent. Furthermore, the results show that eco-routing produces reductions in HC, CO, NO_x, and CO_2 emissions in the range of 37, 41, 43, and 17 percent, respectively. The table also shows the average speed of both routing options. The average speed for TT-routing, 86.4 km/h (or 54 mph) is slightly lower than the speed limit (96 km/h or 60 mph) of the interstate highway sections. In case of the eco-routing algorithm, the average trip speed is 44 km/h (or 27.5 mph) while the speed limit of the local road sections is mostly 48 km/h (or 30 mph).

Table 3: Impact of Eco-Routing for a Specific O-D Pair

	TT-routing	Eco-routing
Travel Distance (km)	9.83	7.22
Travel Time (s)	409.41	590.85
Average Speed (km/h)	86.41	44.00
Fuel (l)	1.09	0.89
HC (g)	5.25	3.31
CO (g)	134.35	79.30
NO_x (g)	3.70	2.12
CO_2 (g)	2340.61	1947.79

The previous case showed that eco-routing effectively improved the fuel economy of vehicles on the network. However, the study also found that eco-routing does enhance fuel efficiency in most cases but in some limited cases it actually results in higher fuel consumption levels. Figure 7 illustrates two O-D pairs that were tested and did not produce the desired outcome.

(a) Case 1

(b) Case 2

Figure 7: Vehicle Routing Practice for Sample O-D Pairs (Source – 2012 Google Map)

Table 4 demonstrates the simulation results for two O-D pairs. For the Case 1 scenario, the eco-routing system increased the fuel consumption by 0.7 % compared to the TT-routing system while the eco-routing reduced the fuel consumption by 0.9% for the Case 2 scenario. It is interesting to note that both routing options resulted in routes with similar travel distances, travel times, and average speeds. The results demonstrate that for these cases the fuel-efficient and minimum travel time routes are practically identical. Specifically, in the Case 1 scenario, approximately 90% of the eco-routing vehicles utilize the same highway route that the TT-routing vehicles use, as illustrated in Figure 7 (a), while only 10% of eco-routing vehicles use the arterial route (eco-route). Because of the dynamic nature of the routing algorithm, routing decisions are updated using the real-time road conditions. Table 2 demonstrates that for the Case 1 scenario, the eco-routing option results in longer travel times. The increased travel time is attributed to the 10% of vehicles that utilize the arterial route. For the Case 2 scenario, all eco-routing vehicles use the same route as the TT-routing vehicles. It is noted that because of the stochastic nature of the microscopic traffic simulation marginal differences are observed.

Table 4: Impacts of Routing Options for Sample O-D Pairs

	Case 1		Case 2	
	TT-routing	Eco-routing	TT-routing	Eco-routing
Travel Distance (km)	8.41	8.42	14.38	14.38
Travel Time (s)	402.96	425.33	511.21	513.05
Average Speed (km/h)	75.15	71.23	101.26	100.90
Fuel (l)	0.91	0.92	1.33	1.31
HC (g)	3.90	3.90	3.15	2.93
CO (g)	105.16	103.64	80.96	74.81
NOx (g)	2.84	2.78	4.71	4.64
CO_2 (g)	1979.54	1993.99	2974.49	2956.61

Eco-Routing – All-or-Nothing Comparison

This base scenario investigates the benefit of eco-routing assuming that all vehicles on the network either attempt to minimize their travel time (TT-routing) or minimize their fuel consumption (eco-routing). One-hour demands were loaded and simulated until all vehicles cleared the network and the results were compared considering average MOEs. A single vehicle type (ORNL composite vehicle type) was utilized for the analysis. Figure 8 compares the average fuel consumption, travel distance, and travel time per vehicle for the two test networks. It should be noted that a white noise error (normal distribution with a coefficient of variation equal to 10 percent) was introduced in order to replicate the typical margin of error in travel time and fuel consumption estimation.

As illustrated in Figure 8, eco-routing vehicles effectively save fuel for both the Cleveland and Columbus networks. The figure shows that the average fuel savings for the Cleveland and Columbus networks is 3.98 % and 6.2 %, respectively. In the case of the Columbus network the vehicle fuel consumption level is higher than that for the Cleveland network. This is due to the fact that the size of the Columbus network is larger than the Cleveland network. Figure 8 also shows the average travel distance and travel time for the eco-routing and non-eco-routing vehicles. It shows that the eco-routing vehicles typically use shorter distance but longer travel time routes when compared to the TT-routing vehicles. In particular, the eco-routing system reduces the travel distance by 5.18 and 5.53 percent for the Cleveland and Columbus networks, respectively. The results also demonstrate that eco-routing results in a 4.8 and 3.21 percent increase in the average travel time for the Cleveland and Columbus networks, respectively. For this specific scenario, the eco-routing effectively reduces vehicle fuel consumption with the cost of slightly increasing the travel time.

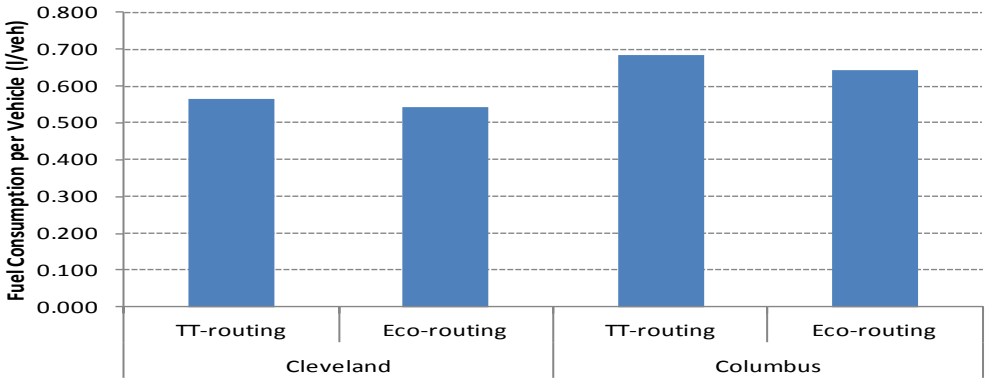

(a) Fuel Consumption

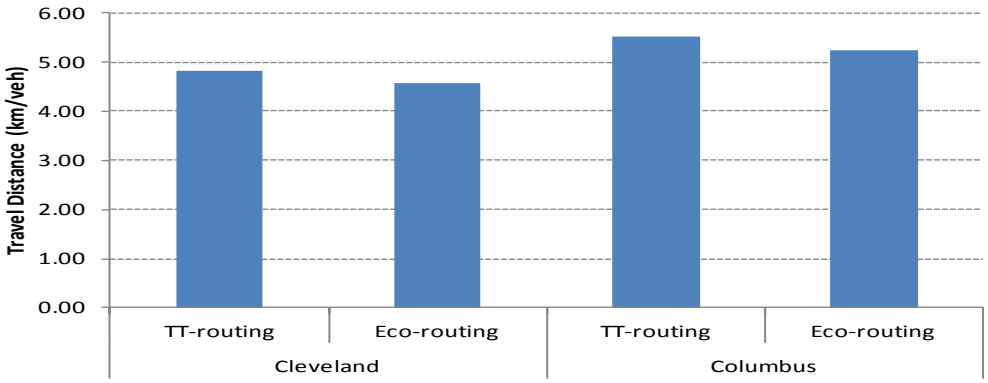

(b) Travel Distance

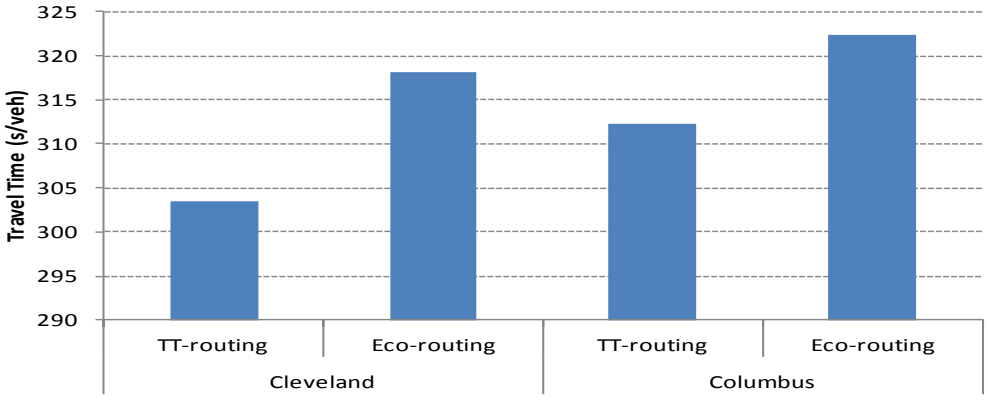

(c) Travel Time

Figure 8: Effects of Eco-routing.

Eco-Routing – Market Penetration Analysis

This section investigates the impact of various levels of market penetration of eco-routing vehicles on the overall transportation system performance, as illustrated in Figure 9. The 10

percent eco-routing represents a 10 percent level of market penetration of eco-routing vehicles with the other 90 percent of vehicles being routed to minimize their travel time (i.e., the traditional TT-routing method). Additionally, 100 percent eco-routing implies that all vehicles on the network utilize the eco-routing algorithm while the matching non-eco-routing values represent the case where all vehicles use TT-routing.

As illustrated in Figure 9, the simulation results demonstrate somewhat different trends for the Cleveland and Columbus networks. The most notable finding is that the eco-routing option does not always result in overall fuel consumption savings for these vehicles, as demonstrated in the case of the Cleveland network. Specifically, the results demonstrate that eco-routing increases the eco-routing vehicles fuel consumption level in most cases except for a few (10 percent and 100 percent eco-routing). The results demonstrate that the eco-routing system results in an increase in the fuel consumption level in the range of 1.57 percent. Alternatively, the simulation results for the Columbus network are more promising. Figure 9 shows that the eco-routing system generally reduces the vehicle fuel consumption levels when compared to the TT-routing scenario regardless of the proportion of the eco-routing vehicles travelling on the network. In particular, the eco-routing system results in overall fuel consumption savings in the range of 4.02 percent relative to standard TT-routing.

This study also quantifies the impact of an eco-routing system on the network-wide travel times considering different LMPs. As shown in Figure 9, the travel time patterns do not match the fuel consumption patterns. Furthermore, the travel time trends differ across the two networks. In particular, in case of the Cleveland network, the eco-routing vehicles spend marginally more travel time (4 seconds) relative to TT-routing vehicles. Interestingly, on the Columbus network the eco-routing system reduces the network-wide time for all LMPs except for the 100 percent LMP scenario. Overall the results demonstrate that TT-routing is highly correlated with fuel consumption levels (0.92 and 0.6 for the Cleveland and Columbus networks, respectively), however eco-routing shows a negative correlation between the travel time and fuel consumption levels (-0.89 for Cleveland and -0.88 for Columbus). In other words, the two objectives (travel time and fuel consumption) are not aligned.

The impact of the routing strategy on the system-wide travel distance is presented in Figure 9. The results show that the travel distance patterns are closely related to the fuel consumption patterns. The correlation coefficient between travel distance and fuel consumption ranges between 0.93 to 0.99 for Cleveland and Columbus networks, respectively. However, a careful examination of the graph reveals that differences are observed for fuel consumption and travel distance objective functions. In particular, for the 10 and 20 percent LMP on the Cleveland network, an increase in the fuel consumption level is produced with a decrease in the travel distance when compared to the TT-routing scenario. However, there are considerable similarities between the relative fuel consumption differences and the relative travel distance differences for the Columbus network.

The simulation results demonstrate that the network configuration has a significant impact on the benefits of eco-routing. The difference in results for the two networks is attributed to the unique features of each network. As mentioned earlier, the I-90 freeway diagonally traverses the Cleveland network. I-90 is the major highway of Cleveland that connects the other interstate highways and runs through the downtown area. On the other hand, the Columbus network is grid-like. Thus it appears that the vehicles on the Columbus network may have more options to re-route when compared to vehicles on the Cleveland

network. Finally, the simulation results indicate that the LMP of eco-routing vehicles significantly impacts the fuel consumption level of individual vehicles.

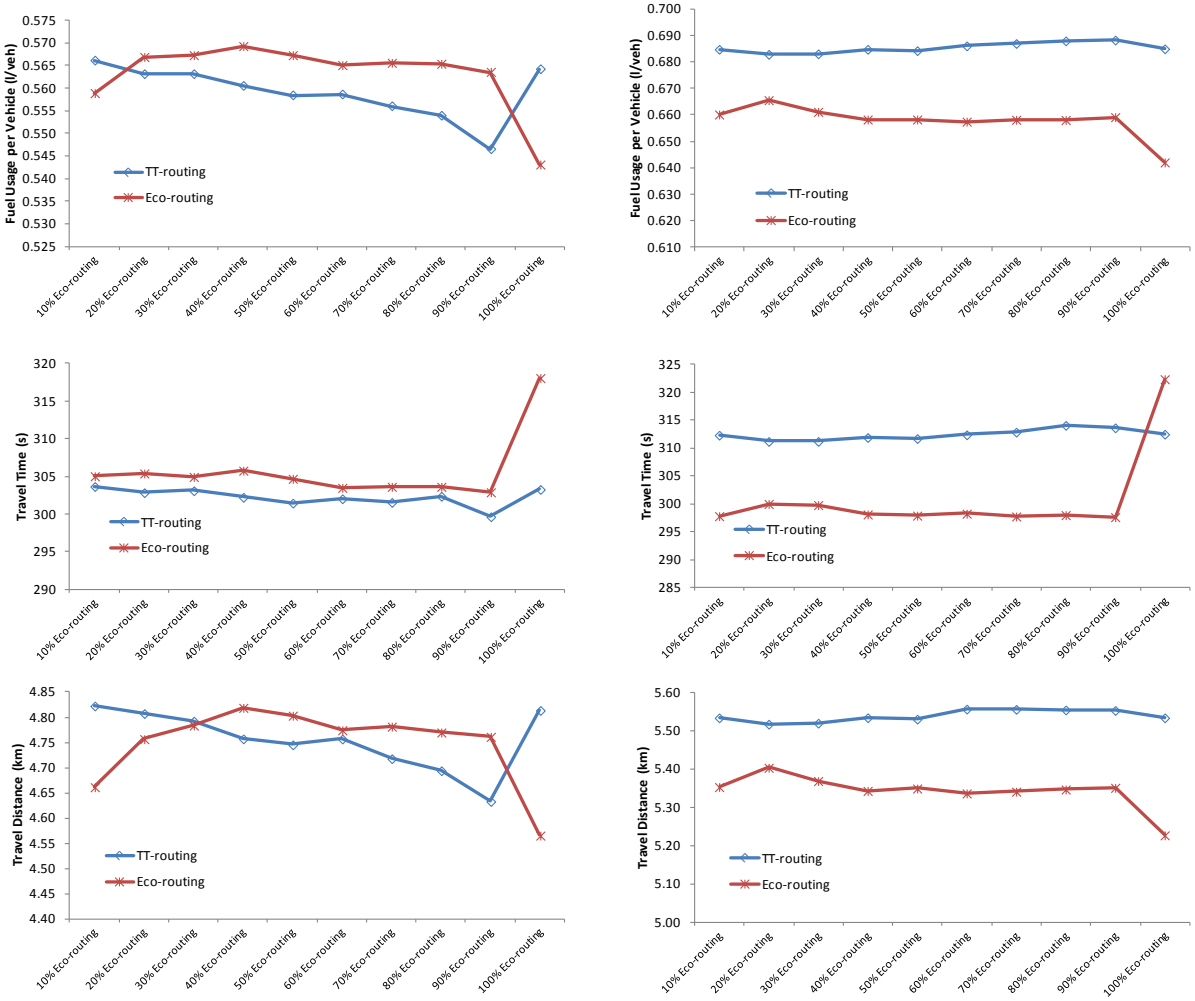

(a) Cleveland (b) Columbus

Figure 9: Market Penetration Impacts on Results.

Traffic Demand Impacts on System Performance

In this section the impact of eco-routing on overall network performance as a function of the network level of congestion is studied. Given that the network-wide congestion level would affect the performance of such systems, the study attempts to identify a range of congestion levels in which eco-routing strategies can be effective. To quantify the impacts of various congestion levels, the traffic demand was varied using uniform scaling factors of 0.25, 0.50, 1.50 and 2.00.

Figure 10 compares the average fuel consumption of an individual vehicle for various congestion levels for different LMPs for the Cleveland and Columbus networks. The simulation results demonstrate that the fuel consumption savings for eco-routing vehicles are highly dependent on the level of congestion. In the case of the Cleveland network, the

simulation results indicate that the eco-routing option generally reduces the fuel consumption for the eco-routing vehicles as shown in the figure except for a few cases. In particular, the average fuel savings of the eco-routing vehicles on the Cleveland network are 2.22%, 1.43%, 0.17%, and 1.29% for the 25, 50, 150, and 200 percent demand levels, respectively. However, in some cases, the eco-routing option results in increased network-wide fuel consumption levels relative to the TT-routing option. These increases are very minor (0.1 percent or less). However, in one case the eco-routing vehicle fuel consumption increased by 1.49 percent compared to TT-routing (10 percent eco-routing scenario at 150 percent demand level).

The figure also shows that, excluding the 150 percent demand level, the eco-routing vehicles save more fuel when a small percentage of eco-routing vehicles are deployed on the network. In particular, in the 50% demand level on the Cleveland network, the eco-routing vehicles produce a 3.1 percent reduction in the network-wide fuel consumption level when compared to a 10 to 40 percent LMP while the average fuel saving for the other cases is only 0.32 percent.

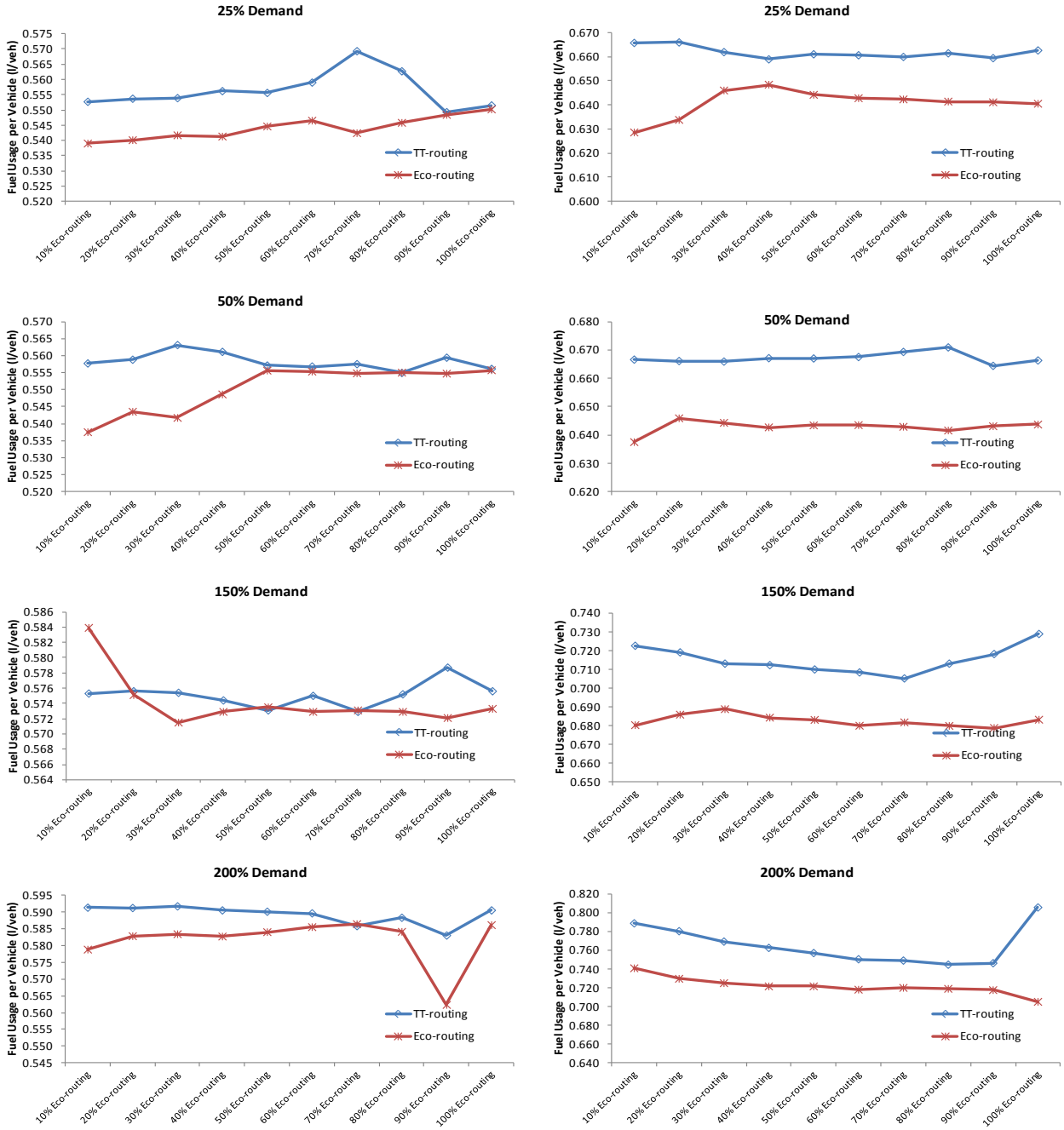

(a) Cleveland (b) Columbus

Figure 10: Impacts of Various Congestion Levels.

In the case of the Columbus network, eco-routing always results in fuel consumption savings relative to TT-routing for all congestion levels, as demonstrated in Figure 10. The average fuel savings for the eco-routed vehicles on the Columbus network are 3.14%, 3.63%, 4.53%, and 5.63% for the 25, 50, 150 and 200 percent demand levels, respectively. Interestingly, in the case of the Columbus network the benefits of eco-routing increase with an increase in the level of congestion. It is hypothesized that these benefits are attributable to

the grid nature of the Columbus roadway network. The figure also shows the impact of an eco-routing system for low congestion levels (25% the original peak demand). The simulation results demonstrate that in the case of the Cleveland network the fuel savings for eco-routing is higher for the lower demand levels. These results are reversed in the case of the Columbus network. These differences in findings can be attributed to the network structure. As mentioned previously, in the case of downtown Cleveland, I-90 runs diagonally and thus there appear to be fewer alternative routes; however, at low traffic demands the non-freeway roadways are more fuel efficient. Since the downtown is a grid-shaped in the case of the Columbus network low congestion levels do not provide better alternatives for eco-routing vehicles.

Vehicle Type Impacts on Eco-routing Performance

Figure 11 quantifies the network-wide impact of an eco-routing system considering two different vehicle types: a fuel efficient vehicle that uses less fuel than the average vehicle under normal driving conditions and the ORNL average vehicle. Detailed descriptions of the fuel efficient and low-emitting (LDV3) vehicles are provided in the literature [42]. In this case the 50 percent original demand level was considered. The figure clearly illustrates that fuel efficient vehicles consume significantly less fuel than the less efficient vehicles. In particular, when the fuel efficient vehicles are used, the average eco-routing and TT-routing vehicles incur savings of approximately 32 and 34 percent for the Cleveland and Columbus networks, respectively.

The simulation results indicate that the fuel efficient vehicles incur larger fuel savings on the Columbus network compared to the Cleveland network when the eco-routing option is adopted. These results are consistent with the results when using the ORNL composite vehicle. It is interesting to note that the fuel consumption trends for the fuel efficient vehicles are similar to the trends of the original scenario vehicles for both the Cleveland and Columbus networks. Specifically, the eco-routing option produces fuel savings of 0.61% and 3.28% for the Cleveland and Columbus networks, respectively. The finding demonstrates that the eco-routing system appears to produce similar savings regardless of the vehicle type considered in the analysis.

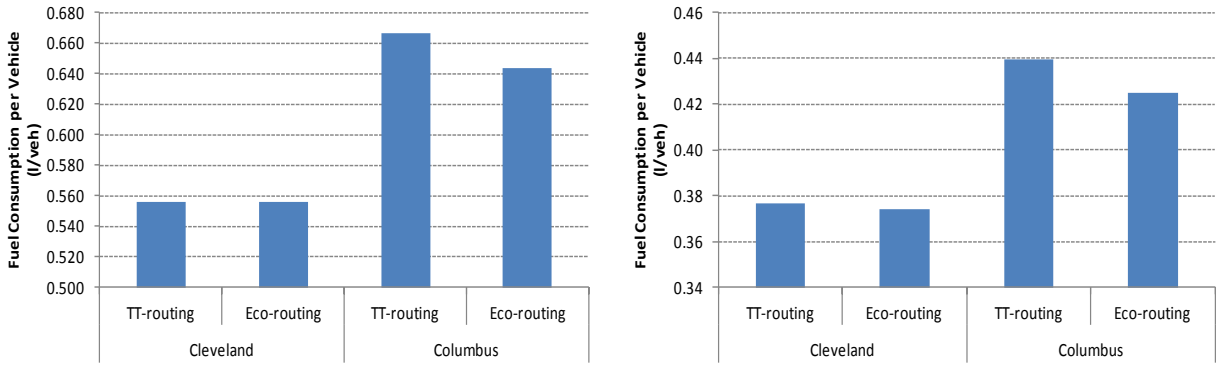

(a) ORNL Composite Vehicle (b) Fuel Efficient Vehicles

Figure 11: Impacts of eco-routing for fuel efficient vehicles.

Eco-Routing – System-wide Impacts

Figure 12 illustrates the system-wide impacts of eco-routing strategies within the Cleveland and Columbus networks. In particular, the results compare the total fuel consumption and average travel time for variable demand scenarios with different market penetrations of the eco-routing system. Figure 12 shows that the total fuel consumption increases as the total demand level increases due to the higher total vehicle miles traveled.

The figure demonstrates that the network-wide results are network dependent. The results from the Cleveland network show inconsistent patterns while the results from the Columbus network demonstrate a downward trend as the proportion of eco-routing vehicles increases for both the total fuel consumed and the average trip travel time. In the case of the Cleveland network, a careful examination of the graph demonstrates that the eco-routing system does not affect the system-wide fuel consumption level and the trip travel time significantly for most cases except for the very congested case (twice the peak demand). More specifically, in the case of the Cleveland network peak demand the differences in total fuel consumed and average travel time are negligibly small and are less than one percent regardless of the percentage of the eco-routing vehicles traversing the network. Thus, it is safe to claim that in the case of the Cleveland network eco-routing have minimum system-wide impacts.

Figure 12 also shows the simulation results for the Columbus network. The results clearly demonstrate network-wide reductions in the fuel consumption level as a function of the level of market penetration. Specifically, as the portion of eco-routing vehicles increase, the network-wide fuel consumption level is reduced by up to 3.3%, 3.4%, 3.8%, 6.3% and 11.9% for the 25%, 50%, 100%, 150%, and 200% peak demand scenarios, respectively. The results seem to demonstrate that the savings in fuel consumption levels increase as the level of congestion increases. Furthermore, the results demonstrate that both network-wide travel times and fuel consumption levels are aligned. The eco-routing appears to shift the UE assignments towards the SO assignment and thus produces reductions in the total travel time over the network

As was demonstrated earlier, the eco-routing vehicles incur largest fuel savings when a small percentage of the fleet is equipped with the eco-routing system (10 to 30%). However, when analyzing the entire system-wide impacts, larger levels of eco-routing system penetration produce larger system-wide fuel consumption in most cases. Consequently, even though eco-routing vehicles cannot reduce their fuel consumption levels when the LMP exceeds 30%, they contribute to further reductions of fuel consumption levels for other vehicles.

Figure 13 illustrates the overall fuel consumption per vehicle for different eco-routing strategies. The fuel consumption values represent the average value of all simulation scenarios. For example, the value for 90 percent eco-routing of the Cleveland network corresponds to the average fuel consumption value per vehicle for the total system-wide fuel consumption values for all demand levels (25, 50, 100, 150, and 200 percent) when 90 percent of the vehicles are eco-routed and 10 percent are travel time routed. The simulation results demonstrate that the deployment of 90 percent and 100 percent eco-routing vehicles effectively reduces the fuel consumption of individual vehicles on the Cleveland and the Columbus networks for all demand levels.

Figure 13 also includes the combined average fuel consumption of the Cleveland and Columbus networks. The combined results show that the system-wide fuel consumption benefits can be achieved when all eco-routing vehicles are assigned to the network.

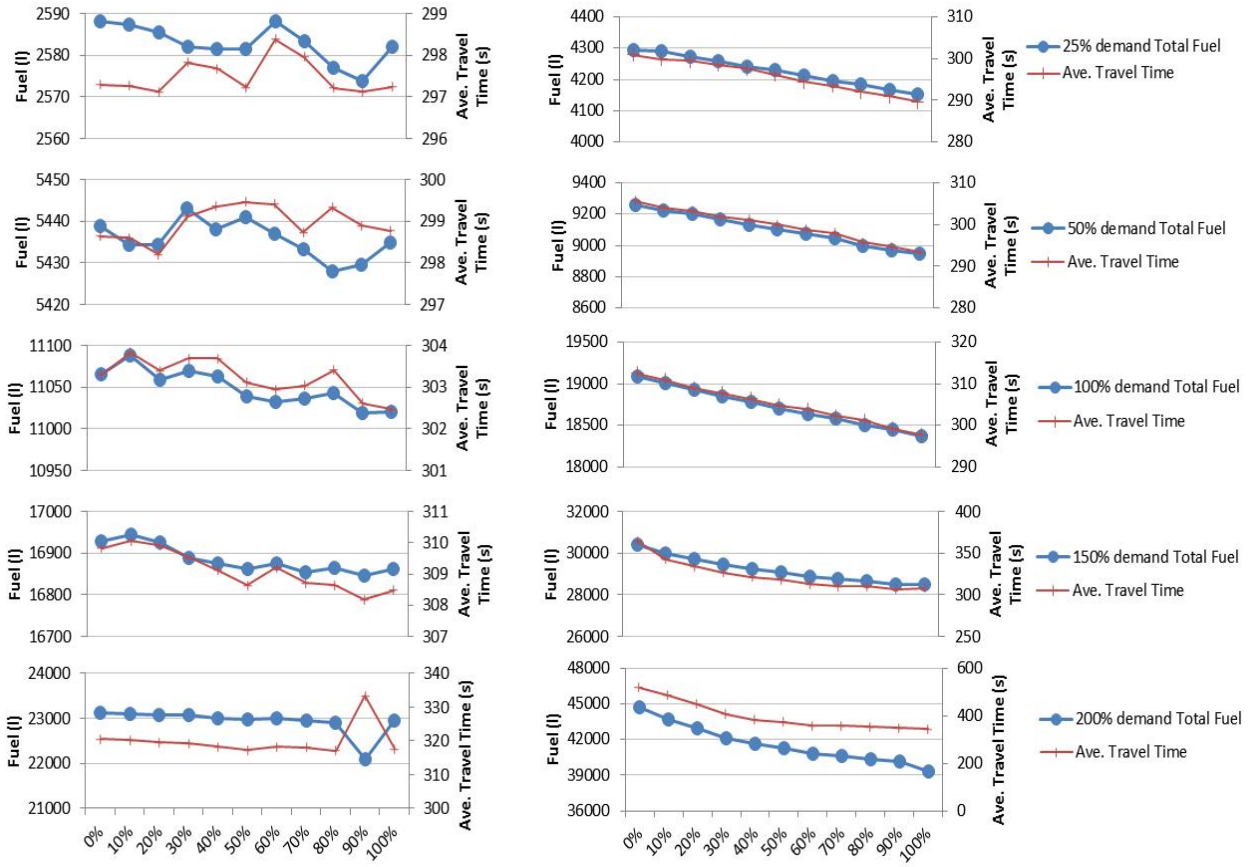

(a) Cleveland (b) Columbus

Figure 12: System-wide Impacts of Eco-routing for Various Congestion Levels.

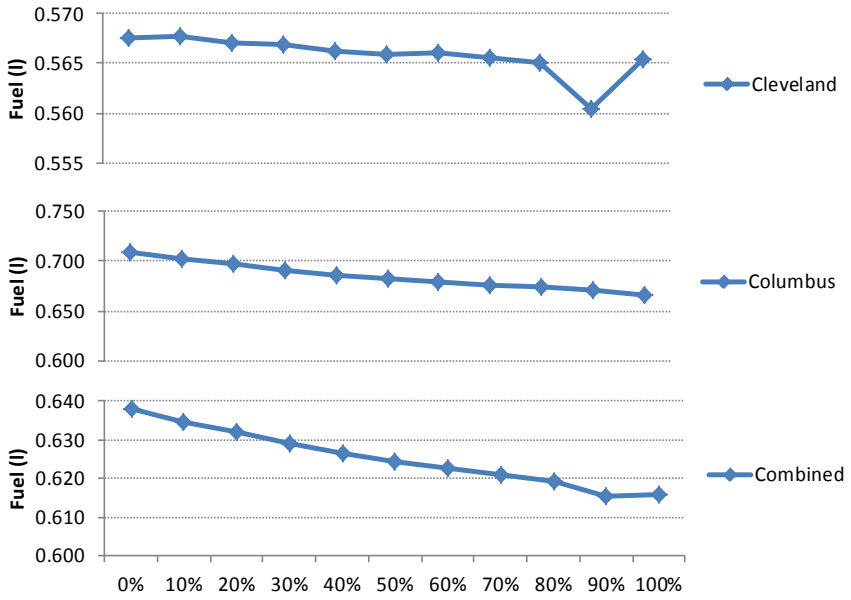

Figure 13: Combined Network-wide Impacts of Eco-routing.

Conclusions

The study presented eco-routing modeling and strategies. Two eco-routing algorithms are developed: one based on vehicle sub-populations (ECO-Subpopulation Feedback Assignment or ECO-SFA) and another based on individual drivers (ECO-Individual Feedback Assignment or ECO-IFA). Both approaches initially assign vehicles based on fuel consumption levels for travel at the facility free-flow speed. Subsequently, fuel consumption estimates are refined based on experiences of other vehicles within the same class. This stochastic, multi-class, dynamic traffic assignment framework was demonstrated to work for two Scenarios.

This study also quantifies the system-wide impacts of implementing a dynamic eco-routing system, considering various levels of market penetration and levels of congestion in downtown Cleveland and Columbus, Ohio, USA. The study concludes that eco-routing systems can reduce network-wide fuel consumption and emission levels in most cases; the fuel savings over the networks range between 3.3% and 9.3% when compared to typical travel time minimization routing strategies. We demonstrate that the fuel savings achieved through eco-routing systems are sensitive to the network configuration and level of market penetration of the eco-routing system. The results also demonstrate that an eco-routing system typically reduces vehicle travel distance but not necessarily travel time. We also demonstrate that the configuration of the transportation network is a significant factor in defining the benefits of eco-routing systems. Specifically, eco-routing systems appear to produce larger fuel savings on grid networks compared to freeway corridor networks. The study also demonstrates that different vehicle types produce similar trends with regard to eco-routing strategies. Finally, the system-wide benefits of eco-routing generally increase with an increase in the level of the market penetration of the system.

REFERENCES

[1] G. H. Tzeng and C. H. Chen, "Multiobjective Decision-Making for Traffic Assignment," *Ieee Transactions on Engineering Management,* vol. 40, pp. 180-187, May 1993.

[2] C. M. Benedek and L. R. Rilett, "Equitable traffic assignment with environmental cost functions," *Journal of Transportation Engineering-Asce,* vol. 124, pp. 16-22, Jan-Feb 1998.

[3] L. R. Rilett and C. M. Benedek, "Traffic assignment under environmental and equity objectives," *Transportation Research Record,* pp. 92-99, 1994.

[4] S. Sugawara and D. A. Niemeier, "PART 2 - AIR QUALITY - How Much Can Vehicle Emissions Be Reduced? Exploratory Analysis of an Upper Boundary Using an Emissions-Optimized Trip Assignment," *Transportation research record,* p. 9, 2002 2002.

[5] A. Nagurney, "Congested urban transportation networks and emission paradoxes," *Transportation Research, Part D: Transport & Environment,* vol. 5, pp. 145-151, 2000.

[6] A. Nagurney, P. Ramanujam, and K. K. Dhanda, "Multimodal traffic network equilibrium model with emission pollution permits: Compliance vs noncompliance," *Transportation Research, Part D: Transport & Environment,* vol. 3, pp. 349-374, 1998.

[7] A. Nagurney and J. Dong, "A multiclass, multicriteria traffic network equilibrium model with elastic demand," *Sage Urban Studies Abstracts,* vol. 30, pp. 415-517, 2002 2002.

[8] K. Ahn and H. Rakha, "The Effects of Route Choice Decisions on Vehicle Energy Consumption and Emissions," *Transportation Research Part D: Transport and Environment,* vol. 13, pp. 151-167, 2008.

[9] M. Van Aerde and S. Yagar, "Dynamic Integrated Freeway/Traffic Signal Networks: A Routeing-Based Modelling Approach," *Transportation Research,* vol. 22A(6), pp. 445-453, 1988.

[10] M. Van Aerde and S. Yagar, "Dynamic Integrated Freeway/Traffic Signal Networks: Problems and Proposed Solutions," *Transportation Research,* vol. 22A(6), pp. 435-443, 1988.

[11] M. Van Aerde and H. Rakha, "INTEGRATION © Release 2.40 for Windows: User's Guide – Volume I: Fundamental Model Features," M. Van Aerde & Assoc., Ltd., Blacksburg2012.

[12] M. Van Aerde and H. Rakha, "INTEGRATION © Release 2.40 for Windows: User's Guide – Volume II: Advanced Model Features," M. Van Aerde & Assoc., Ltd., Blacksburg2012.

[13] H. Rakha, I. Lucic, S. H. Demarchi, J. R. Setti, and M. Van Aerde, "Vehicle dynamics model for predicting maximum truck acceleration levels," *Journal of Transportation Engineering,* vol. 127, pp. 418-425, 2001.

[14] H. Rakha and I. Lucic, "Variable power vehicle dynamics model for estimating maximum truck acceleration levels," *Journal of transportation engineering,* vol. 128, pp. 412-419, 2002.
[15] H. Rakha and Y. Zhang, "INTEGRATION 2.30 framework for modeling lane-changing behavior in weaving sections," *Transportation Research Record.,* pp. 140-149, 2004.
[16] H. Rakha, K. Ahn, and K. Moran, "INTEGRATION Framework for Modeling Eco-routing Strategies: Logic and Preliminary Results," *International Journal of Transportation Science and Technology (IJTST),* vol. 1, pp. 259-274, 2012.
[17] M. Van Aerde and H. Rakha, "INTEGRATION © Release 2.30 for Windows: User's Guide – Volume I: Fundamental Model Features," M. Van Aerde & Assoc., Ltd., Blacksburg2007.
[18] M. Van Aerde and H. Rakha, "INTEGRATION © Release 2.30 for Windows: User's Guide – Volume II: Advanced Model Features," M. Van Aerde & Assoc., Ltd., Blacksburg2007.
[19] H. Rakha, A. Medina, H. Sin, F. Dion, M. Van Aerde, and J. Jenq, "Traffic signal coordination across jurisdictional boundaries: Field evaluation of efficiency, energy, environmental, and safety impacts," *Transportation Research Record,* vol. n 1727, pp. 42-51 2000.
[20] H. Rakha, Y.-S. Kang, and F. Dion, "Estimating vehicle stops at undersaturated and oversaturated fixed-time signalized intersections," *Transportation Research Record,* vol. n 1776, pp. 128-137 2001.
[21] F. Dion, H. Rakha, and Y.-S. Kang, "Comparison of delay estimates at under-saturated and over-saturated pre-timed signalized intersections," *Transportation Research Part B-Methodological,* vol. 38, pp. 99-122, 2004.
[22] H. Rakha, M. Van Aerde, K. Ahn, and A. A. Trani, "Requirements for evaluating traffic signal control impacts on energy and emissions based on instantaneous speed and acceleration measurements," *Transportation Research Record,* vol. n 1738, pp. 56-67 2000.
[23] H. Rakha, K. Ahn, and A. Trani, "Development of VT-Micro model for estimating hot stabilized light duty vehicle and truck emissions," *Transportation Research, Part D: Transport & Environment,* vol. 9, pp. 49-74, 2004.
[24] K. Ahn, H. Rakha, A. Trani, and M. Van Aerde, "Estimating vehicle fuel consumption and emissions based on instantaneous speed and acceleration levels," *Journal of Transportation Engineering,* vol. 128, pp. 182-190, 2001.
[25] K. Ahn, H. Rakha, and A. Trani, "Microframework for modeling of high-emitting vehicles," *Transportation Research Record. ,* pp. 39-49, 2004.
[26] A. Avgoustis, H. Rakha, and M. Van Aerde, "Framework for estimating network-wide safety Impacts of intelligent transportation systems," in *Intelligent Transportation Systems Safety and Security Conference* Miami, 2004.
[27] H. Rakha and B. Crowther, "Comparison of Greenshields, Pipes, and Van Aerde car-following and traffic stream models," *Transportation Research Record. ,* pp. 248-262 2002.

[28] H. Rakha and B. Crowther, "Comparison and calibration of FRESIM and INTEGRATION steady-state car-following behavior," *Transportation Research,* vol. 37A, pp. 1-27, 2003.
[29] H. Rakha, "An Evaluation of the Benefits of User and System Optimised Route Guidance Strategies," M.Sc., Civil Engineering, Queen's University, Kingston, 1990.
[30] H. Rakha, A. M. Flintsch, K. Ahn, I. El-Shawarby, and M. Arafeh, "Evaluating alternative truck management strategies along interstate 81," *Transportation Research Record,* vol. n 1925, pp. 76-86, 2005.
[31] H. Rakha, M. Van Aerde, L. Bloomberg, and X. Huang, "Construction and calibration of a large-scale microsimulation model of the Salt Lake area," *Transportation Research Record,* vol. n 1644, pp. 93-102, 1998.
[32] S. Park and H. Rakha, "Energy and Environmental Impacts of Roadway Grades," *Transportation Research Record,* vol. 1987, pp. 148-160, 2006.
[33] H. Rakha, K. Ahn, and A. Trani, "Microscopic modeling of vehicle start emissions," *Transportation Research Record. ,* pp. 29-38 2003.
[34] L. R. Rilett, M. Van Aerde, G. Mackinnon, and M. Krage, "Simulating the TravTek route guidance logic using the integration traffic model," in *Vehicle Navigation & Information Systems Conference Proceedings Part 2 (of 2)*, Dearborn, MI, USA, 1991, pp. 775-787.
[35] L. R. Rilett and M. W. van Aerde, "Modelling distributed real-time route guidance strategies in a traffic network that exhibits the Braess paradox," in *Vehicle Navigation & Information Systems Conference Proceedings Part 2 (of 2)*, Dearborn, MI, USA, 1991, pp. 577-587.
[36] L. Rilett and M. Van Aerde, "Routing based on anticipated travel times," in *Proceedings of the 2nd International Conference on Applications of Advanced Technologies in Transportation Engineering*, Minneapolis, MN, USA, 1991, pp. 183-187.
[37] L. Rilett and V. Aerde, "Modeling Route Guidance Using the Integration Model," in *Proceedings of the Pacific Rim Trans Tech Conference*, Seattle, WA, USA, 1993, pp. 258-264.
[38] H. Rakha and Y. Zhang, "Analytical procedures for estimating capacity of freeway weaving, merge, and diverge sections," *Journal of Transportation Engineering,* vol. 132, pp. 618-628, 2006.
[39] H. Rakha and K. Ahn, "Integration modeling framework for estimating mobile source emissions," *Journal of transportation engineering,* vol. 130, pp. 183-193, 2004 2004.
[40] K. Ahn, H. Rakha, A. Trani, and M. Van Aerde, "Estimating vehicle fuel consumption and emissions based on instantaneous speed and acceleration levels," *Journal of Transportation Engineering-Asce,* vol. 128, pp. 182-190, Mar-Apr 2002.
[41] K. Ahn, H. Rakha, A. Trani, and M. Van Aerde, "Estimating vehicle fuel consumption and emissions based on instantaneous speed and acceleration levels," *Journal of Transportation Engineering,* vol. 128, pp. 182-190, 2002.
[42] H. Rakha, K. Ahn, and A. Trani, "Development of VT-Micro model for estimating hot stabilized light duty vehicle and truck emissions," *Transportation Research Part D-Transport and Environment,* vol. 9, pp. 49-74, Jan 2004.